Bioresource Technology 172 (2014) 219–225

Contents lists available at ScienceDirect

Bioresource Technology

journal homepage: www.elsevier.com/locate/biortech

Pyrolysis characteristics of cattle manures using a discrete distributed activation energy model

Hongliang Cao, Ya Xin, Dianlong Wang, Qiaoxia Yuan *

College of Engineering, Huazhong Agricultural University, No. 1, Shizishan Street, Hongshan District, Wuhan 430070, PR China

HIGHLIGHTS

- A discrete DAEM for the pyrolysis process of cattle manures is established.
- The pyrolysis process can be accurately characterized by 27 dominating reactions.
- Complex interaction phenomenon among the constituents of cattle manures is revealed.
- Kinetic parameters for each constituent during the pyrolysis process are obtained.
- Two quantitative relationships are proposed with increasing the heating rate.

ARTICLE INFO

Article history:
Received 13 August 2014
Received in revised form 10 September 2014
Accepted 11 September 2014
Available online 18 September 2014

Keywords:
Cattle manures
Pyrolysis
Distributed activation energy model
Thermogravimetric analysis
Model prediction

ABSTRACT

The pyrolysis characteristics of cattle manures were conducted using a discrete distributed activation energy model (DAEM) coupled with the thermogravimetric analysis. The results showed that the pyrolysis process can be accurately characterized by 27 dominating reactions, and the dominating reactions form four groups to represent respectively the decomposition processes of the different constituents of cattle manures. Moreover, the devolatilization kinetics under the heating rate changing from 0.1 K min^{-1} to 10,000 K min^{-1} were predicted with the discrete DAEM. Prediction results demonstrated that with increasing the heating rate, the main decomposition regions of individual constituent become more and more concentration and their interactions are more and more complex. Particularly, it was interesting to discover that the peak decomposition rate is perfectly proportional to the heating rate, and the peak, starting and ending decomposition temperatures satisfy a relationship of quadratic function with the common logarithm of the heating rate.

1. Introduction

With the increasing cattle feeding operations, cattle manure disposal is becoming a problem because of its increasing production and potential contamination of soil, air, ground and surface water sources by running off from the manure sites and odor releases (Sanchez et al., 2009; Saunders et al., 2012; Venglovsky et al., 2009). Alternative solutions have been proposed by researchers to address the environmental problems, and at the same time to use the renewable and sustainable energy and nutrients within cattle manures. For instance, biochemical, physicochemical, and thermochemical pathways are all possible solutions with different purposes (Huang et al., 2011; Zaks et al., 2011). Thermochemical conversion represents a promising alternative due to the advantages of high temperature elimination of pathogens, drastically reducing waste stream volume, as well as extracting green energy and the production of value-added products (Wu et al., 2013; Zhang et al., 2009).

Thermochemical conversion can be subdivided further into combustion, pyrolysis, and gasification. Combustion is the conversion of chemical energy stored in an organic matter into heat with CO_2 and H_2O as final products in excess air. Pyrolysis, on the other hand, is a conversion process in an oxygen deficient environment, generating volatile products (condensable and non-condensable gases) and solid products (fixed carbon and ash). Gasification falls between complete combustion and pyrolysis, converting organic materials into a combustible gas mixture through partial oxidation (Hayhurst, 2013; Nasir Uddin et al., 2013). Within these thermochemical processes it is fairly interesting to point out that pyrolysis is the less pollutant, for CO_x, SO_x, and NO_x production is reduced compared to combustion and gasification. In addition, pyrolysis

* Corresponding author. Tel./fax: +86 027 87282120.
E-mail address: yc1group@126.com (Q. Yuan).

http://dx.doi.org/10.1016/j.biortech.2014.09.049
0960-8524/

is not only as a single process, but also as a first step to combustion and gasification. Consequently, understanding the characteristics and kinetics of cattle manure pyrolysis is greatly important for the thermochemical disposal of cattle manures.

In this context, considerable studies on the pyrolysis conversion of cattle manures have been addressed with the analytical method of thermogravimetric analysis (TGA) experiments and kinetic models (Wang et al., 2011; Tu et al., 2008; Wu et al., 2012; Ngo et al., 2010; Xu and Chen, 2013). Although much work has been conducted to study cattle manure pyrolysis, extensive research on a definitive mechanism is still the subject of much discussion. For example, a deeper understanding on the pyrolysis process and characteristics by systematically considering the contributions from individual constituent of cattle manures is an interesting issue. Moreover, in a real combustion or gasification process, the heating rate in the pyrolysis step is extremely high, e.g., 10,000 K min^{-1}, due to very high temperatures in the reaction chamber (Bahng et al., 2009; Scott et al., 2006a,b). What is the kinetics of the pyrolysis process under the severe condition has not been reported, due to it is fairly difficult to perform *in situ* measurements and to reproduce in conventional experiment systems. On the other hand, what is the kinetics under the case of extremely low heating rate like 0.1 K min^{-1} is also missing (Bahng et al., 2009). These particular conditions all are vital issues for the design and optimization of thermochemical conversion processes of cattle manures.

Kinetic models are useful means for predicting the kinetics intrinsically related to the pyrolysis mechanisms. More importantly, for the particular conditions as mentioned above, kinetic modeling is very available to gain key data in more accessible conditions to know the particularities of the samples and lately extrapolate to the case of real conditions (Várhegyi et al., 1997; Xu and Chen, 2013). Recently, some exhaustive reviews on kinetic models for biomass pyrolysis have been reported (Cai et al., 2014; Di Blasi, 2008; White et al., 2011). A survey of the reviews shows that numerous kinetic models have been developed, such as single-step global reaction models, multiple-step models, semi-global models, and distributed activation energy model (DAEM), to establish the kinetics of pyrolysis processes. Moreover, different biomass materials show different behavior because of their inherent physicochemical characteristics, which can lead a criterion on the mathematical description selected for its modeling. In this sense, DAEM is considered as an accurate and versatile approach to model the pyrolysis process (Cai et al., 2014; Soria-Verdugo et al., 2013).

The DAEM was originally developed for coal pyrolysis (Pitt, 1962). In the last years, the model has been thoroughly employed to analyze the kinetics of pyrolysis of different biomass feedstocks (Cai et al., 2013; Kirtania and Bhattacharya, 2012; Li et al., 2009; Shen et al., 2011; Sonobe and Worasuwannarak, 2008; Soria-Verdugo et al., 2013, 2014; Yan et al., 2009; Yang et al., 2014). In the DAEM, an infinite number of first order reactions following a given distribution of activation energies and constant pre-exponential factor are assumed. This idea is interesting, however, there is not a physical justification to keep the pre-exponential factor constant and it is clear that there are not an infinite number of reactions. Under this context, Scott et al. (2006a,b) proposed a discrete DAEM, a modified model of the conventional DAEM represented via many (but finite), parallel first-order reactions. The discrete DAEM assume that the complex material is a mixture of different components, each of which decomposes following a first-order reaction characterized uniquely by its characteristic activation energy and pre-exponential factor. For the advantage, the discrete DAEM can identify and characterize the underlying distribution of reactions dominating devolatilization, and provide crucial information on how and when a reaction occurs during pyrolysis process. The authors has successfully applied the discrete DAEM to predict the kinetics of the devolatilization of dried sewage sludge; the results show that the model can provide an accurate description for the kinetics and the number of reactions characterizing the model is far away from infinite (there are no too much). Since the advantages as mentioned above, the discrete DAEM has been successfully and extensively employed for the studies of the pyrolysis kinetics of other materials with volatile content, such as ABS plastic, tyre rubber, coal, petcoke, and wood (Navarro et al., 2008, 2012).

In the present work, the discrete DAEM coupled with the TGA experiment are employed to perform a systematic investigation of the pyrolysis characteristics of cattle manures. The results showed that the pyrolysis process can be accurately characterized by 27 dominating reactions, and the dominating reactions form four groups to represent respectively the contributions from each constituent of cattle manures. The kinetic parameters for individual constituent during the pyrolysis process were obtained, and a complex interaction phenomenon among the constituents was revealed. Furthermore, the prediction results from the model demonstrated that the kinetics under the two particular conditions (heating rate at 0.1 and 10,000 K min^{-1}) have striking difference. With increasing the heating rate, some interesting varying characteristics were discovered. In particular, the quantitative relationships were proposed for the peak decomposition rate and temperature, as well as the starting and ending decomposition temperatures vs. the heating rate during the devolatilisation process. This research gives a deeper insight into the pyrolysis mechanism of cattle manures and provides a useful reference for the design and optimization of its thermochemical disposal.

2. Methods

2.1. Sample preparation

The cattle manure used was collected from the dongzheng feedlot located in Jiangxia District, Wuhan City, Hubei Province, PR China. After being dried, cattle manure samples were crushed and screened to 100 mesh (0.154 mm) size particles. Samples prepared were stored in a closed container to be used for TGA experiments. The moisture content of fresh cattle manure is 84.10 wt%, and the contents of volatile matter, fixed carbon, and ash in dry basis are 64.13, 18.23, and 17.64 wt%, respectively. In addition, the ultimate analysis showed that the cattle manure consists of 36.21 wt% of carbon (C), 5.14 wt% of hydrogen (H), 2.39 wt% of nitrogen (N), 1.32 wt% of sulfur (S), and 54.95 wt% of oxygen (O).

2.2. TGA experiment

TGA experiments of the samples were performed by a simultaneous thermal analyzer (TA SDT Q600) under atmospheric pressure. Samples were heated in the TGA apparatus from ambient temperature to 1073 K with a constant heating rate. Herein four constant heating rates of 5, 10, 20, and 40 K min^{-1} were conducted to prepare experiment data for the identification and validation of the discrete DAEM. For each heating rate, a repeat run of 3 times was done to confirm the results measured.

In all experiments, the carrier gas was ultrahigh purity nitrogen (99.99%) with a constant flow rate of 100 ml min^{-1} and utilized for the purposes of maintaining the inert atmosphere and purging volatiles generated from sample pyrolysis. Moreover, to mitigate the difference of heat and mass transfer, all samples weight were kept approximately at 10 mg. In addition, the thermogravimetric analyzer was purged with the purge gas for 10 min before beginning the heating program, and all TGA runs began with a 30 min isothermal hold at 383 K to drive off the surface moisture and some inherent moisture from the samples.

2.3. Analytical method

The discrete DAEM proposed by Scott et al. (2006a,b) is employed in this research, which is described by the following equation:

$$\frac{M(t)}{M_0} = \omega + \sum_{\text{All reactions},i} f_{i,0} \underbrace{\exp\left[-A_i \int_0^t \exp\left(\frac{-E_i}{RT(t)}\right) dt\right]}_{\psi_i(t)}. \quad (1)$$

where $M(t)$ is the mass of the sample that contains a fraction ω of inert material (fixed carbon and ash), M_0 is the initial value of $M(t)$, $f_{i,0}$ is the fraction of M_0 which decomposes with an activation energy E_i and pre-exponential factor A_i, R is the universal gas constant, $T(t)$ is the temperature, and $\psi_i(t)$ is a double exponential term. Using experimentally measured $M(t)$, the problem is to find $f_{i,0}$, E_i, and A_i.

If the reactions were known, together with E_i and A_i, then Eq. (1) would be a linear problem: the mass of sample remaining at a given time would be the sum of the masses of all components remaining. This implies that Eq. (1) can be rewritten as a matrix equation, where for any set of times t_1, t_2, t_3, etc.,

$$\underbrace{\frac{1}{M_0}\begin{bmatrix} M(t_0) \\ M(t_1) \\ M(t_2) \\ \vdots \end{bmatrix}}_{\underline{M}} = \underbrace{\begin{bmatrix} \psi_1(t_0) & \psi_2(t_0) & \cdots & \psi_n(t_0) & 1 \\ \psi_1(t_1) & \psi_2(t_1) & \cdots & \psi_n(t_1) & 1 \\ \psi_1(t_2) & \psi_2(t_2) & \cdots & \psi_n(t_2) & 1 \\ \psi_1(t_3) & \psi_2(t_3) & \cdots & \psi_n(t_3) & 1 \\ \vdots & \vdots & \ddots & \vdots & 1 \end{bmatrix}}_{\underline{\underline{\Psi}}} \times \underbrace{\begin{bmatrix} f_{1,0} \\ f_{2,0} \\ f_{3,0} \\ \vdots \\ \omega \end{bmatrix}}_{\underline{f}}. \quad (2)$$

Regarding to an experiment with a constant heating rate of $dT/dt = B$, the double exponential term, $\psi_i(t)$, can be written as,

$$\Psi_i(t) = \Psi_i(T) = \exp\left[\frac{-A_i}{B} \int_{T_0}^{T} \exp\left(\frac{-E_i}{RT(t)}\right) dT\right], \quad (3)$$

where T_0 is the initial temperature of the sample. Since there are usually more experimental results than reactions, it is possible to solve Eq. (2) by using linear least squares; each initial mass fraction, $f_{i,0}$, becomes a parameter, which can be evaluated by minimizing the difference between the values of $\underline{M}$ and $\underline{\underline{\Psi}} \times \underline{f}$, subject to the constraint that only positive values of $f_{i,0}$ are allowed. Therefore, each initial mass fraction, $f_{i,0}$, can be calculated by inverting Eq. (2). Here, the *lsqnonneg* function in Matlab (e.g., MATLAB® R2009a, The Mathworks Inc.) is utilized.

In order to calculate $f_{i,0}$ using Eq. (2), a set of reactions must first be generated, each reaction with a known E_i and A_i. Scott et al. (2006a,b) has addressed in detail for the computation of E_i and A_i by,

$$\frac{\frac{1}{B_1}\left[T_0 \exp\left(\frac{-E_i}{RT_0}\right) - \frac{E_i}{R}\int_{E/RT_0}^{\infty} \frac{\exp(-u)}{u} du - T_1 \exp\left(\frac{-E_i}{RT_1}\right) + \frac{E_i}{R}\int_{E/RT_1}^{\infty} \frac{\exp(-u)}{u} du\right]}{\frac{1}{B_2}\left[T_0 \exp\left(\frac{-E_i}{RT_0}\right) - \frac{E_i}{R}\int_{E/RT_0}^{\infty} \frac{\exp(-u)}{u} du - T_2 \exp\left(\frac{-E_i}{RT_2}\right) + \frac{E_i}{R}\int_{E/RT_2}^{\infty} \frac{\exp(-u)}{u} du\right]} = 1, \quad (4)$$

$$\frac{A_i}{B_1}\left[T_0 \exp\left(\frac{-E_i}{RT_0}\right) - \frac{E_i}{R}\int_{E/RT_0}^{\infty} \frac{\exp(-u)}{u} du - T_2 \exp\left(\frac{-E_i}{RT_2}\right) + \frac{E_i}{R}\int_{E/RT_2}^{\infty} \frac{\exp(-u)}{u} du\right] = -1, \quad (5)$$

respectively. For more information on the model, please refer to the work of Scott et al. (2006a,b).

Two experimental sets of data obtained at the heating rates of 10 and 20 K min^{-1} were employed to calculate the distribution of activation energies (E_i) and pre-exponential factors (A_i) by using Eqs. (4) and (5), and then the initial mass fractions ($f_{i,0}$) and the fraction of inert material (ω) were gained via Eq. (2). In the model, the kinetic parameters of E_i and A_i were evaluated at 100 equally spaced intervals of conversion (fraction of sample remaining), corresponding to an unreacted fraction in the range 0.99–0.36.

3. Results and discussion

On the basis of the discrete DAEM established, four theoretical decomposition curves were produced at 5, 10, 20, and 40 K min^{-1}. And then, the theoretical curves were compared with the experimental data measured at the four heating rates to complete a robust test for the model. As shown in Fig. 1, it is observed that the model not only fits perfectly the data used at 10 and 20 K min^{-1}, but also predicts the pyrolysis behavior of the cattle manure samples when the heating rate is increased to 40 K min^{-1} and decreased to 5 K min^{-1}. Notice that for the higher heating rate of 40 K min^{-1}, the model tends to slightly over-predict the pyrolysis process. This over-prediction is due largely to the occurrence of secondary reactions of the primary pyrolysis products as reported by Scott et al. (2006a,b) who suggests that the presence of secondary reactions causes volatile matter cracking resulting in the generation of fixed carbon. The robust test demonstrates that the model is greatly accurate and is an effective tool for predicting the pyrolysis behavior of cattle manures without the disturbance of secondary reactions.

3.1. Pyrolysis characteristics

According to the kinetic parameters derived from the discrete DAEM, the pyrolysis process of cattle manures can be accurately characterized by 27 dominating reactions ($i = 27$), and individual dominating reaction has an initial mass fraction allocated ($f_{i,0}$), as well as a characteristic activation energy (E_i) and pre-exponential factor (A_i). Their distributions vs. the fraction of mass remaining are shown in Fig. 2. For the convenience of discussion, we number the dominating reactions from 1 to 27 along the direction of the decrease of the fraction of mass remaining.

An interesting phenomenon is observed that the dominating reactions tend to form four groups as the decrease of fraction of mass remaining: the first four reactions ($i = 1$–4) form the group I around 0.97, reactions 5 and 6 form the group II around 0.9, reactions 7 and 8 form the group III around 0.73, and the left 19 reactions ($i = 9$–27) form the group IV after 0.56. The phenomenon indicates that the pyrolysis process occurs with four main stages, which are represented respectively by the four reaction groups. This can be explained in the perspective of the constituents of cattle manures (Wu et al., 2012; Xu and Chen, 2013). As reported by Tu et al. (2008), the constituents of cattle manures can be divided

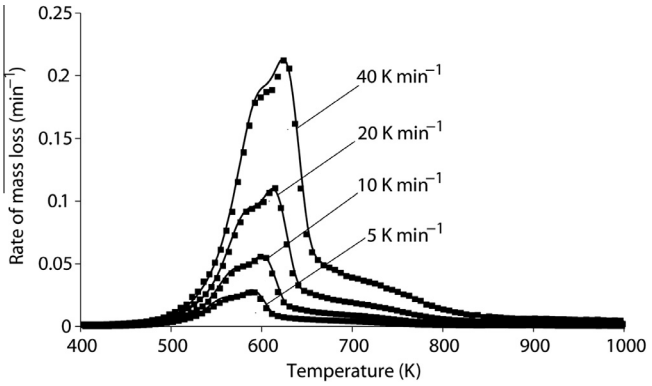

Fig. 1. Comparison of experimental data (blocks) and theoretical decomposition rate curves (solid lines) generated using the discrete distributed activation energy model.

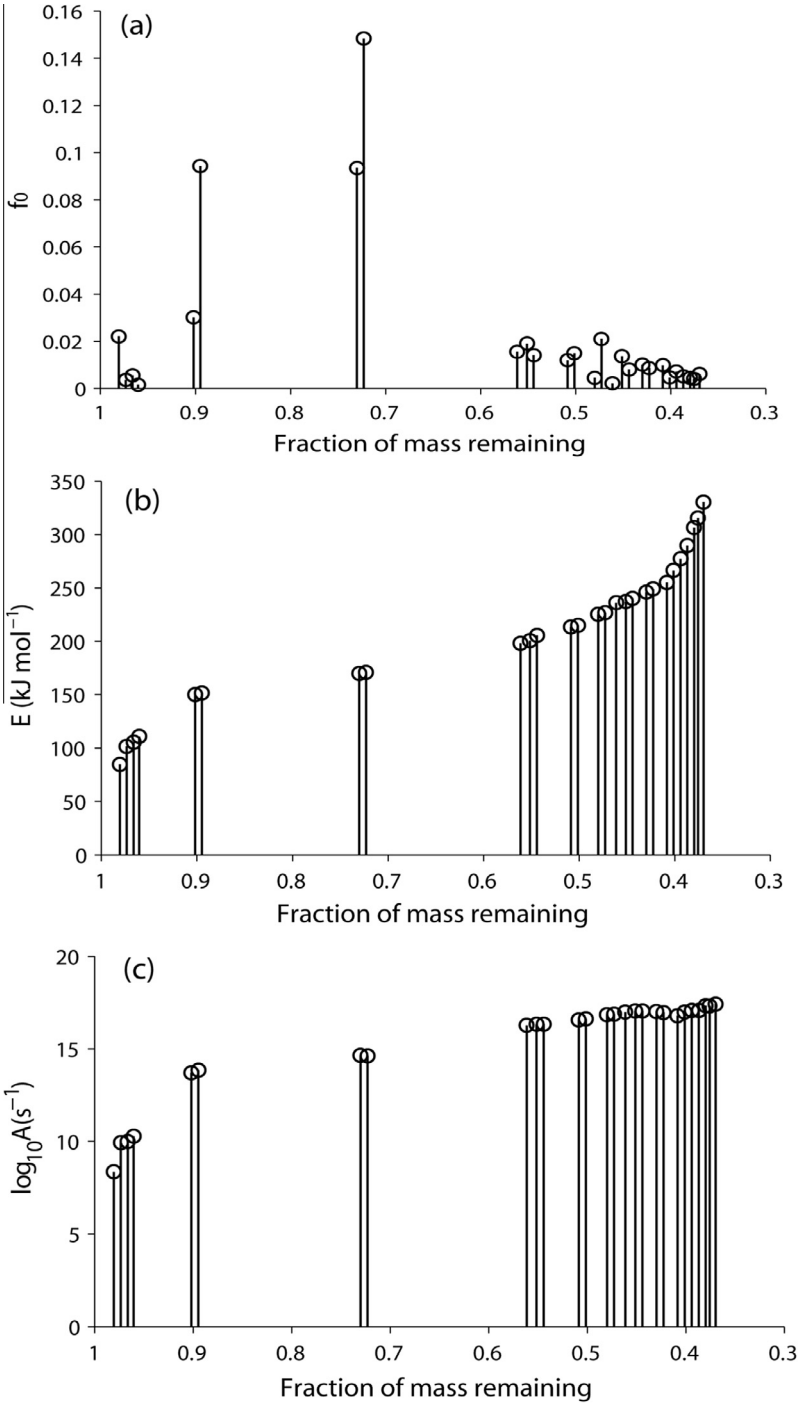

Fig. 2. Distributions of dominating reactions vs. the fraction of mass remaining during the pyrolysis process of cattle manures: (a) initial mass fractions, (b) activation energies, and (c) pre-exponential factors.

into neutral detergent soluble (e.g., proteins, starches, lipids, sugars, etc.), hemicellulose, cellulose, and lignin. Each constituent primarily decompose in different stages for the difference of physicochemical structures. The more complex the structure, the more difficult the decomposition becomes (Caballero et al., 1997; Carrier et al., 2011). In this sense, the group I represents the decomposition of the neutral detergent soluble, the group II represents the hemicellulose, the group III represents the cellulose, and the group IV represents the lignin.

Regarding to the kinetic parameters of the dominating reactions during different decomposition stages, it observed that the neutral detergent soluble has the least activation energies ranging from 84.82 to 110.64 kJ mol^{-1}, and the hemicellulose and cellulose at approximately 150 and 170 kJ mol^{-1}, respectively. The activation energies of the lignin extend through a broad interval from 198.25 to 330.48 kJ mol^{-1}, which demonstrates the lignin has a much complex structure than the other constituents and has an extremely wide activity range for the chemical bonds and functional groups. This complex mechanism of the lignin decomposition is also justified from the quantity of the dominating reactions (including 19 reactions). Like in that case, the distribution of the pre-exponential factors has a closely related behavior

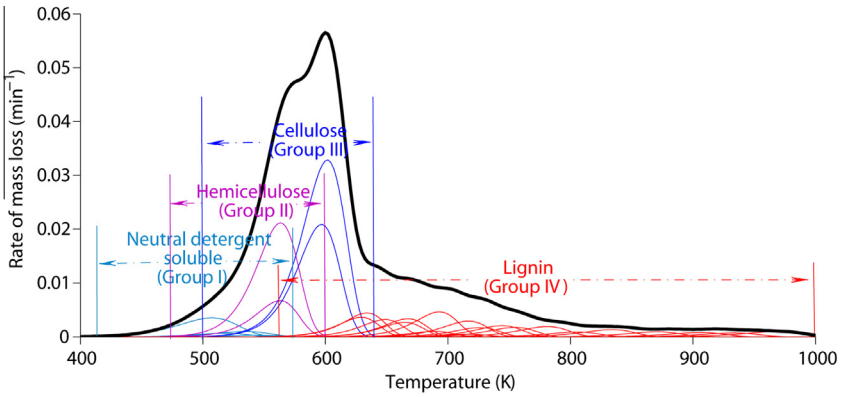

Fig. 3. Pyrolysis process of cattle manures under the heating rate of 10 K min^{-1}. Thin lines represent the pyrolysis process of the constituents and the thick line is the composition of the thin lines, representing the pyrolysis process of cattle manures.

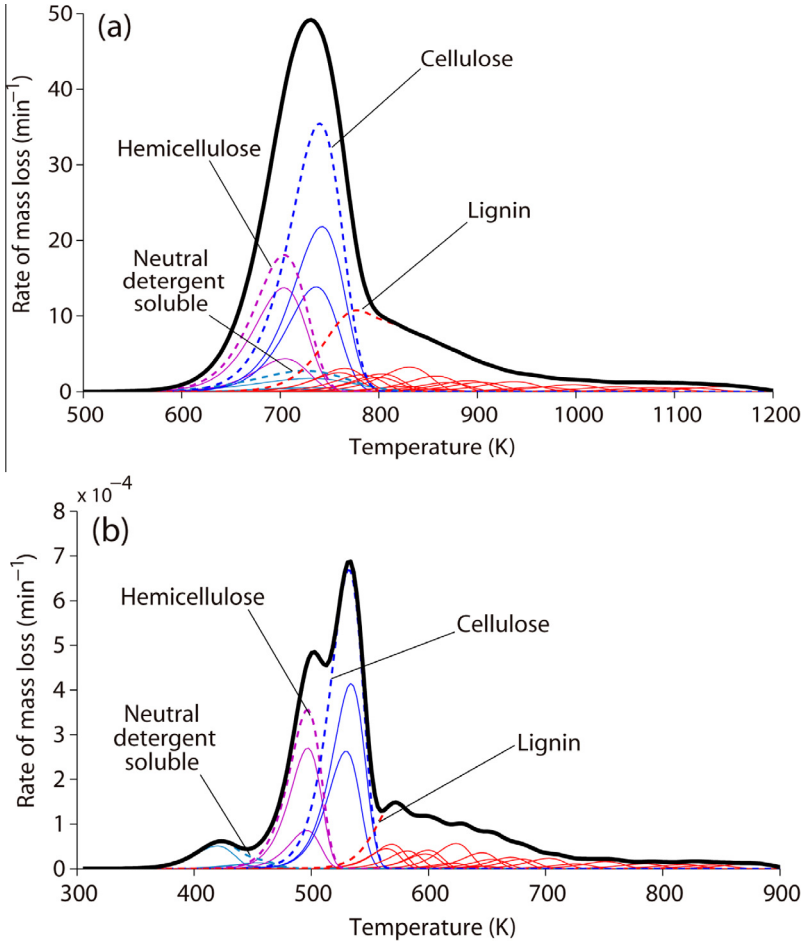

Fig. 4. Pyrolysis process of cattle manures under the two particular cases: (a) heating rate at 10,000 K min^{-1}, and (b) heating rate at 0.1 K min^{-1}.

to the distribution of the activation energies. This relationship satisfies the "compensation effect" (Hayhurst, 2013), in so far as when the activation energy is increased from 84.82 to 330.48 kJ mol^{-1}, the pre-exponential factor increases hugely from 2.27×10^8 to 2.67×10^{17} s^{-1}. The distribution of the kinetic parameters is in good agreement with the complexities of the chemical composition of cattle manures.

In Fig. 3, the pyrolysis process and characteristics contributed from the different constituents are clearly displayed. Here we take for example the case that the heating rate is 10 K min^{-1}. As discussed above, the neutral detergent soluble is thermally most sensitive and is the first one beginning to decompose as the increase of temperatures. The degradation of the neutral detergent soluble mainly takes place around 512 K with a starting decomposition temperature of 410 K, and the degradation process is completed around 580 K. After about 60 K from the starting decomposition temperature of the neutral detergent soluble, the hemicellulose starts to decompose, and the decomposition rate reaches the maximum value around 563 K. With increasing further the operating temperature, the decomposition of the hemicellulose

almost is completed at 600 K. While around the temperature of 600 K, the cellulose is decomposing with the maximum rate of mass loss. The starting and ending decomposition temperatures of the cellulose are 500 and 640 K, respectively. Finally, the lignin has a broad decomposition region from 560 to 1000 K due to its complex physicochemical structure. During the pyrolysis process, it is obvious that the decomposition regions of the constituents overlap each other, which clearly demonstrates there are complex interactions among the constituents.

3.2. Kinetics prediction

Here, we conduct the pyrolysis behavior for the particular cases as discussed in Section 1 under the heating rates at 10,000 and 0.1 K min^{-1}, respectively. As shown in Fig. 4(a), when the heating rate is increased to 10,000 K min^{-1}, the maximum decomposition peak becomes very high, e.g., 49.16 min^{-1}, and the decomposition rate curve has an obvious shift to higher temperatures compared with the mild case (see Fig. 3). Moreover, the shoulder peak on the left of the main peak disappears and only a large single peak is displayed for the decomposition rate curve. In this case, the neutral detergent soluble, hemicellulose, and cellulose almost have the same starting decomposition temperatures, e.g., 580 K, and the lignin at 660 K; the peak decomposition temperatures of the four constituents are 727, 704, 740, and 778 K, respectively. These peak decomposition temperatures are obtained by composing the decomposition rate curves of the corresponding dominating reactions of the constituents. Notice that the peak decomposition temperature of the neutral detergent soluble is lager than that of the hemicellulose, meaning that the primary degradation region of the neutral detergent soluble falls behind that of the hemicellulose; even the primary degradation range of the neutral detergent soluble is the same as that of the cellulose. It is obvious that the main decomposition regions for the constituents become more concentration and the interactions among the constituents are more and more complex as the increase of heating rates.

On the other hand, when the heating rate is decreased to 0.1 K min^{-1}, the pyrolysis behavior is shown in Fig. 4(b). In this case, the maximum decomposition peak is only 6.87×10^{-4} min^{-1}, and the decomposition rate curve has an obvious shift to lower temperatures compared with the mild and high heating rates (see Figs. 3 and 4(a)). Furthermore, a high resolution image of the pyrolysis process is generated where the decomposition peaks for the constituents can be identified clearly. For example, the first decomposition peak is produced by the neutral detergent soluble, the second one by hemicellulose, the third one by cellulose, and the left obscure peaks by lignin. In this sense, the main decomposition regions for the constituents become looser and the interaction among the constituents becomes weaker and weaker as the decrease of heating rates.

As discussed above the heating rate affects strongly the pyrolysis kinetics, such as the peak decomposition rate and the corresponding peak decomposition temperature as well as the starting and ending decomposition temperatures during pyrolysis processes. These typical indexes are essential to the design and optimization of the thermochemical conversion processes. Consequently, we systematically address these indexes with the heating rate increasing from 0.1 to 10,000 K min^{-1} on the basis of the discrete DAEM.

It is interesting to find that the peak decomposition rate is perfectly proportional to the heating rate as shown in Fig. 5(a). In the Fig. 5(a), since the heating rates cover a very wide range from 0.1 to 10,000 K min^{-1}, we have taken a common (base 10) logarithm for both the peak decomposition rate and the heating rate to more clearly display the results. Moreover, the three decomposition temperatures also have perfect kinetic behavior with the

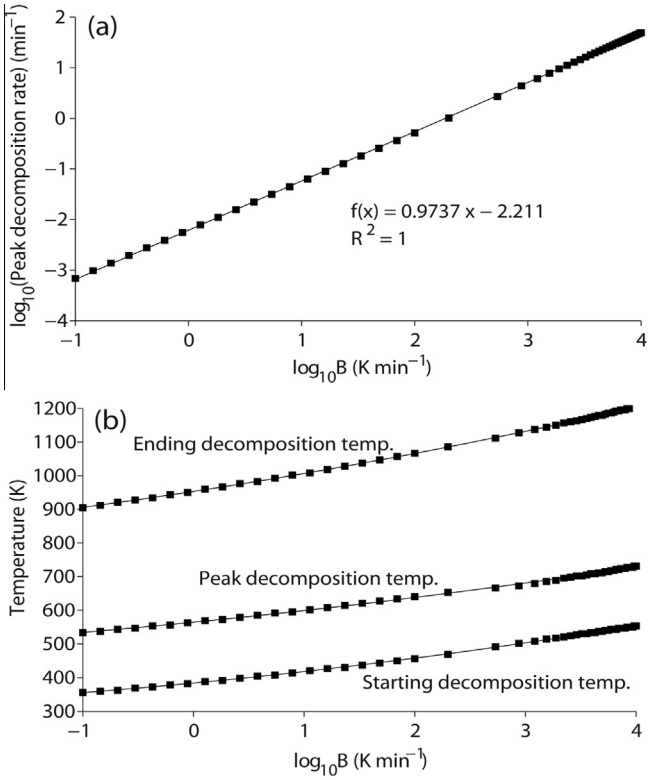

Fig. 5. Four typical indexes during pyrolysis processes vs. the heating rate: (a) peak decomposition rate, and (b) peak, starting, and ending decomposition temperatures. Blocks represent the predicted data from the discrete DAEM and solid lines are fitting curves generated using the Curve Fitting Tool in Matlab (MATLAB® R2009a, The Mathworks Inc.).

increase of heating rates, as shown in Fig. 5(b), subject to a relationship of quadratic function as follows:

$$T = ax^2 + bx + c, \tag{6}$$

where x denotes the common logarithm of heating rates ($x = \log_{10} B$), and a, b, and c denote the parameters of the quadratic function (see Table 1).

According to the proportional relationship (see Fig. 5(a)), it is easy to estimate the maximum rate of mass loss at any given heating rate. The maximum rate of mass loss is of vital importance to industries that use cattle manure in applications such as gasification or combustion. Where gasification is concerned, the maximum rate of mass loss for the cattle manure sample at individual representative heating rate indicates the maximum yield of volatiles. Furthermore, the peak, starting, and ending decomposition temperatures for the devolatilization process can be accurately predicted on the basis of the quadratic function relationship of Eq. (6), and the time taken to achieve these key temperature points also can be easily gained through the heating rate of B K min^{-1}. These quantitative relationships are important guideline for the design and optimization of thermochemical conversion processes

Table 1
Model parameters of the peak, starting, and ending decomposition temperatures.

Temperatures (K)	a	b	c	R^2
T_{peak}	2.121	32.39	564.7	0.9989
T_{sta}	2.787	31.31	384.3	0.9997
T_{end}	3.109	50.23	953.1	0.9999

T_{peak}, peak decomposition temperature; T_{sta}, starting decomposition temperature; T_{end}, ending decomposition temperature; R^2, correlation coefficient.

of cattle manures. Notice that the predicted results, using the discrete DAEM, have a hypothesis that the devolatilization process mainly considers first-order reactions, neglecting the influence of secondary reactions during the pyrolysis process. Therefore, the predicted results will have a certain amount of error with the real devolatilization process, but they are good references for real applications. In future work, it is necessary to pay an attention on the influence of secondary reactions, particularly for the cases of high heating rates, to reveal more accurately the real process.

4. Conclusions

The pyrolysis characteristics of cattle manures were addressed in detail by the discrete DAEM coupled with TGA experiments. The pyrolysis behavior can be accurately characterized by 27 dominating reactions, and the dominating reactions form four groups to represent respectively the decomposition processes of the four constituents of cattle manures. Moreover, as the increase of heating rates, the main decomposition regions for the constituents become more and more concentration and their interactions are more and more complex. More importantly, two quantitative relationship expressions are proposed for the peak decomposition rate and the key decomposition temperature points vs. the heating rate.

Acknowledgements

This research was financially supported by the Special Fund for Agro-scientific Research in the Public Interest (201303091) and the Fundamental Research Funds for the Central Universities (52902-0900206116). Moreover, the authors want to thank Ashok Pandey, Editor, Bioresource Technology, and anonymous reviewers for their help and suggestion.

References

Bahng, M., Mukarakate, C., Robichaud, D.J., Nimlos, M.R., 2009. Current technologies for analysis of biomass thermochemical processing: a review. Anal. Chim. Acta 651, 117–138.

Caballero, J.A., Conesa, J.A., Font, R., Marcilla, A., 1997. Pyrolysis kinetics of almond shells and olive stones considering their organic fractions. J. Anal. Appl. Pyrol. 42, 159–175.

Cai, J., Wu, W., Liu, R., Huber, G.W., 2013. A distributed activation energy model for the pyrolysis of lignocellulosic biomass. Green Chem. 15, 1331–1340.

Cai, J., Wu, W., Liu, R., 2014. An overview of distributed activation energy model and its application in the pyrolysis of lignocellulosic biomass. Renew. Sustain. Energy Rev. 36, 236–246.

Carrier, M., Loppinet-Serani, A., Denux, D., Lasnier, J., Ham-Pichavant, F., Cansell, F., Aymonier, C., 2011. Thermogravimetric analysis as a new method to determine the lignocellulosic composition of biomass. Biomass Bioenergy 35, 298–307.

Di Blasi, C., 2008. Modeling chemical and physical processes of wood and biomass pyrolysis. Prog. Energy Combust. Sci. 34, 47–90.

Hayhurst, A.N., 2013. The kinetics of the pyrolysis or devolatilisation of sewage sludge and other solid fuels. Combust. Flame 160, 138–144.

Huang, Y.F., Kuan, W.H., Chiueh, P.T., Lo, S.L., 2011. A sequential method to analyze the kinetics of biomass pyrolysis. Bioresour. Technol. 102, 9241–9246.

Kirtania, K., Bhattacharya, S., 2012. Application of the distributed activation energy model to the kinetic study of pyrolysis of the fresh water algae *Chlorococcum humicola*. Bioresour. Technol. 107, 476–481.

Li, Z., Liu, C., Chen, Z., Qian, J., Zhao, W., Zhu, Q., 2009. Analysis of coals and biomass pyrolysis using the distributed activation energy model. Bioresour. Technol. 100, 948–952.

Nasir Uddin, M., Daud, W.M.A.W., Abbas, H.F., 2013. Potential hydrogen and non-condensable gases production from biomass pyrolysis: insights into the process variables. Renew. Sustain. Energy Rev. 27, 204–224.

Navarro, M.V., Aranda, A., Garcia, T., Murillo, R., Mastral, A.M., 2008. Application of the distributed activation energy model to blends devolatilisation. Chem. Eng. J. 142, 87–94.

Navarro, M.V., Martínez, J.D., Murillo, R., García, T., López, J.M., Callén, M.S., Mastral, A.M., 2012. Application of a particle model to pyrolysis. Comparison of different feedstock: plastic, tyre, coal and biomass. Fuel Process. Technol. 103, 1–8.

Ngo, T., Kim, J., Kim, S., 2010. Characteristics and kinetics of cattle litter pyrolysis in a tubing reactor. Bioresour. Technol. 101, S104–S108.

Pitt, G.J., 1962. The kinetics of the evolution of volatile products from coal. Fuel 41, 267–274.

Sanchez, M.E., Otero, M., Gómez, X., Morán, A., 2009. Thermogravimetric kinetic analysis of the combustion of biowastes. Renewable Energy 34, 1622–1627.

Saunders, O.E., Fortuna, A., Harrison, J.H., Cogger, C.G., Whitefield, E., Green, T., 2012. Gaseous nitrogen and bacterial responses to raw and digested dairy manure applications in incubated soil. Environ. Sci. Technol. 46, 11684–11692.

Scott, S.A., Dennis, J.S., Davidson, J.F., Hayhurst, A.N., 2006a. An algorithm for determining the kinetics of devolatilisation of complex solid fuels from thermogravimetric experiments. Chem. Eng. Sci. 61, 2339–2348.

Scott, S.A., Dennis, J.S., Davidson, J.F., Hayhurst, A.N., 2006b. Thermogravimetric measurements of the kinetics of pyrolysis of dried sewage sludge. Fuel 85, 1248–1253.

Shen, D.K., Gu, S., Jin, B., Fang, M.X., 2011. Thermal degradation mechanisms of wood under inert and oxidative environments using DAEM methods. Bioresour. Technol. 102, 2047–2052.

Sonobe, T., Worasuwannarak, N., 2008. Kinetic analyses of biomass pyrolysis using the distributed activation energy model. Fuel 87, 414–421.

Soria-Verdugo, A., Garcia-Hernando, N., Garcia-Gutierrez, L.M., Ruiz-Rivas, U., 2013. Analysis of biomass and sewage sludge devolatilization using the distributed activation energy model. Energy Convers. Manage. 65, 239–244.

Soria-Verdugo, A., Garcia-Gutierrez, L.M., Blanco-Cano, L., Garcia-Hernando, N., Ruiz-Rivas, U., 2014. Evaluating the accuracy of the distributed activation energy model for biomass devolatilization curves obtained at high heating rates. Energy Convers. Manage. 86, 1045–1049.

Tu, D., Dong, H., Shang, B., 2008. Pyrolysis behavior of selected manures using TG-FTIR techniques livestock environment VIII. In: Proceedings of the International Symposium.

Várhegyi, G., Antal Jr., M.J., Jakab, E., Szabó, P., 1997. Kinetic modeling of biomass pyrolysis. J. Anal. Appl. Pyrol. 42, 73–87.

Venglovsky, J., Sasakova, N., Placha, I., 2009. Pathogens and antibiotic residues in animal manures and hygienic and ecological risks related to subsequent land application. Bioresour. Technol. 100, 5386–5391.

Wang, L., Shahbazi, A., Hanna, M.A., 2011. Characterization of corn stover, distiller grains and cattle manure for thermochemical conversion. Biomass Bioenergy 35, 171–178.

White, J.E., Catallo, W.J., Legendre, B.L., 2011. Biomass pyrolysis kinetics: a comparative critical review with relevant agricultural residue case studies. J. Anal. Appl. Pyrol. 91, 1–33.

Wu, H., Hanna, M.A., Jones, D.D., 2012. Thermogravimetric characterization of dairy manure as pyrolysis and combustion feedstocks. Waste Manage. Res. 30, 1066–1071.

Wu, H., Hanna, M.A., Jones, D.D., 2013. Life cycle assessment of greenhouse gas emissions of feedlot manure management practices: land application versus gasification. Biomass Bioenergy 54, 260–266.

Xu, Y., Chen, B., 2013. Investigation of thermodynamic parameters in the pyrolysis conversion of biomass and manure to biochars using thermogravimetric analysis. Bioresour. Technol. 146, 485–493.

Yan, J.H., Zhu, H.M., Jiang, X.G., Chi, Y., Cen, K.F., 2009. Analysis of volatile species kinetics during typical medical waste materials pyrolysis using a distributed activation energy model. J. Hazard. Mater. 162, 646–651.

Yang, X., Zhang, R., Fu, J., Geng, S., Cheng, J.J., Sun, Y., 2014. Pyrolysis kinetic and product analysis of different microalgal biomass by distributed activation energy model and pyrolysis–gas chromatography–mass spectrometry. Bioresour. Technol. 163, 335–342.

Zaks, D.P.M., Winchester, N., Kucharik, C.J., Barford, C.C., Paltsev, S., Reilly, J.M., 2011. Contribution of anaerobic digesters to emissions mitigation and electricity generation under U.S. climate policy. Environ. Sci. Technol. 45, 6735–6742.

Zhang, S., Hong, R., Cao, J., Takarada, T., 2009. Influence of manure types and pyrolysis conditions on the oxidation behavior of manure char. Bioresour. Technol. 100, 4278–4283.